

## Prediction of material thickness on dome of geodesic wound orthotropic composite vessel

Dinh Van Hien\*, Tran Ngoc Thanh

Institute of Missile, Academy of Military Science and Technology;

\*Corresponding author: vanhiencompany221182@gmail.com.

Received 2 Sep 2022; Revised 28 Oct 2022; Accepted 7 Nov 2022; Published 18 Nov 2022.

DOI: <https://doi.org/10.54939/1859-1043.j.mst.83.2022.95-102>

### ABSTRACT

*Orthotropic composite pressure vessels are designed based on considering the role of a matrix in the force balance of the structure and its leakage due to matrix failure. To be more specific, the stress and strain states of the shell are considered simultaneously in both longitudinal and transverse directions of the fiber. Due to such a loaded condition, the laminate thickness prediction of the shell does not use the maximum stress criterion as with the traditional monotropic composite vessels but rather the multi-axial failure criterion of the composite material. With the developed and published platforms on the design of the dome profile of the composite vessel, this paper focuses on predicting the laminate thickness of the geodesic wound dome of the pressure vessel according to Tsai-Wu failure criteria, simultaneously the material thickness distribution on the dome as a basis for determining structural parameters of the vessels.*

**Keywords:** Laminate thickness; Composite pressure vessel; Orthotropic composite; Geodesic winding.

### 1. INTRODUCTION

The design and manufacture of the composite pressure shell of revolution have been developed over the years. For a cylindrical composite vessel with two domes, the structural design problem revolves around two main issues: 1- determining the dome profile to ensure a balanced shape and 2- finding the layer thickness to ensure durability, thereby serving as a premise for determining the winding processing parameters. According to the mathematical description of the fiber trajectory, there are two winding types: geodesic winding and non-geodesic winding, where the geodesic winding is a technique of spreading the fiber on the shell surface, which under the action of fiber tension, the transverse force acting on the fiber is zero, i.e., the fiber has no tendency to slip.

Normally, to determine the dome profile, it is assumed that the composite material is monotropic. When loaded, the material is subjected to tensile stress that is uniformly distributed along the fiber axis and equally in all fibers. This approach is called the *netting theory*. However, in practice, continuous fiber-reinforced composites always exhibit orthotropy. In order to get closer to the actual behavior of the material, the *continuum theory* (lamination theory) has been developed to determine the dome profile, typically as reported by Liang et al. (2002) [1], Vasiliev (2003) [2], Zu et al. (2010) [3], Hien and Thanh (2021) [4] for geodesic and non-geodesic wound composite pressure vessels.

To estimate the laminate thickness, a suitable strength criterion should be used. Some biaxial failure criteria for orthotropic lamina that have been studied are 1- the maximum stress criterion; 2- the maximum strain criterion; 3- Tsai–Hill failure criterion; and 4- Tsai–Wu failure criterion. In fact, the failure of a composite pressure vessel generally includes two main steps: firstly, cracks appear in the matrix, and then the pressure is

taken up by the fibers until they fail [5]. Matrix failure is a serious issue for the safety of a pressure vessel. However, no interaction exists between the failure modes in the maximum stress and strain criterion. Meanwhile, there are certainly some faults in the orthotropic lamina with the Tsai–Hill failure criterion [6]. To avoid both tensile failures transverse to fibers and shear failure along fibers, the design against the failure is determined by employing the Tsai–Wu tensor failure criterion. This failure theory is a relatively new multi-axial strength theory. Specific merits of the Tsai–Wu failure criterion include: 1- invariance under rotation or redefinition of coordinates; 2- transformation via known tensor transformation laws; and 3- symmetry properties akin to those of stiffness and compliances [6]. Tsai-Wu criterion has been widely applied to predict the failure of composite pressure vessels by many authors.

To apply new theories to the design of composite shells of revolution, in this paper, we focus on developing the Tsai-Wu failure criteria to predict the composite layer thickness of the dome of the pressure vessel. In addition, the prediction of material thickness distribution on the dome is also developed in order to approach the actual distribution to serve the design problem accurately.

## 2. THEORETICAL BACKGROUND

### 2.1. Review of building geodesic dome profile

#### 2.1.1. Geometry and physics of filament wound dome

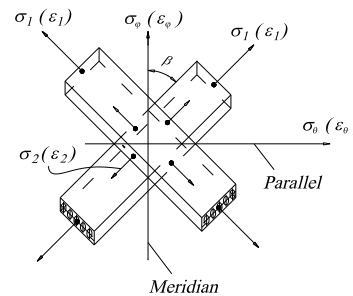
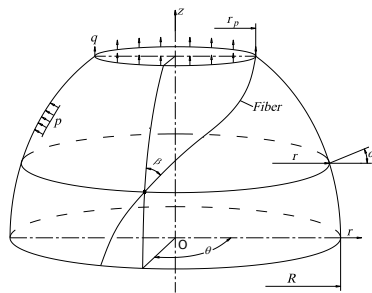


**Figure 1.** The geometry of a dome shell of revolution. **Figure 2.** Stress-strain components in shell element.

Consider a dome surface of revolution  $S(z, \theta) = [z, r(z)\cos\theta, r(z)\sin\theta]^T$  with  $z$ , the axial coordinate,  $\theta$ , the angular coordinate and  $r$ , the radial coordinate as described in Fig. 1. Some main characteristic parameters are as follows:

- $R$  and  $r_p$  are the radial radii of the dome equator and the polar hole;
- $\beta$  is the winding angle (angle between the fiber and meridian of the dome);
- $p$  and  $q$  are the internal pressure and the force on length unit at the polar hole,  $q = p.r_p/2$  for the closed polar hole and  $q = 0$  for the opened polar hole.

#### 2.1.2. Geodesic winding condition

Geodesic winding involves having windings go along the shortest distance between two points on the winding surface to ensure structural stability, that is, no slipping and no bending between the filaments and the winding surface. The geodesic condition is satisfied as follows [1-4]:

$$r \cdot \sin\beta = r_p \tag{1}$$

2.1.3. Stress components and optimum condition of dome profile

- Stresses in meridian and parallel directions based on membrane theory [4, 7]:

$$\sigma_{\varphi} = \frac{\bar{N}_{\varphi}}{h} = \frac{p \cdot \bar{r} \cdot \sqrt{1 + \bar{r}'^2}}{2 \cdot \bar{h}} \left( 1 - C_p \cdot \frac{\bar{r}_p^2}{\bar{r}^2} \right) \quad (2)$$

$$\sigma_{\theta} = \frac{\bar{N}_{\theta}}{h} = \frac{p \cdot \bar{r} \cdot \sqrt{1 + \bar{r}'^2}}{2 \cdot \bar{h}} \left[ 2 + \frac{\bar{r} \cdot \bar{r}''}{1 + \bar{r}'^2} \left( 1 - C_p \cdot \frac{\bar{r}_p^2}{\bar{r}^2} \right) \right] \quad (3)$$

where the subscripts  $\varphi$  and  $\theta$  denote the meridional and parallel direction of the dome, respectively;  $\bar{N}$  is the dimensionless force resultants;  $h$  is the material thickness;  $\bar{r}$ ,  $\bar{r}_p$ ,  $\bar{z}$ ,  $\bar{h}$  are the dimensionless parameters  $\bar{r} = r / R$ ,  $\bar{r}_p = r_p / R$ ,  $\bar{z} = z / R$ ,  $\bar{h} = h / R$ ;  $\bar{r}'$  and  $\bar{r}''$  are the first and second derivatives of  $\bar{r}$  with respect to  $\bar{z}$ ;  $C_p = 0$  or  $1$  is for the dome with the closed or opened polar hole, respectively.

- Stress components based on classical laminate theory: The description of stress components in the composite element of the shell is as in Fig. 2. Since the shell and applied load are axially symmetric, the shear stresses and strains in the meridian and parallel direction must be equal to zero. Thus, we have the following relations [8]:

$$\sigma_{\varphi} = \sigma_1 \cdot \cos^2 \beta + \sigma_2 \cdot \sin^2 \beta - \tau_{12} \cdot \sin 2\beta \quad (4)$$

$$\sigma_{\theta} = \sigma_1 \cdot \sin^2 \beta + \sigma_2 \cdot \cos^2 \beta + \tau_{12} \cdot \sin 2\beta \quad (5)$$

where subscripts 1 and 2 denote the longitudinal and transverse direction of the filament fibers;  $\sigma$  and  $\tau$  denote normal and shear stresses.

2.1.4. Equations of geodesic dome profile

- Governing equation of geodesic dome profile: Based on the stress balance, the condition of the equal shell strains, and the geodesic condition (1), the governing equation of the geodesic dome profile is determined as follows [4]:

$$\bar{r}'' = \left[ \frac{1}{\bar{r}} \cdot \left( \frac{k \cdot \bar{r}^2 + (1-k) \cdot \bar{r}_p^2}{\bar{r}^2 + (k-1) \cdot \bar{r}_p^2} - \frac{2 \cdot \bar{r}^2}{\bar{r}^2 - C_p \cdot \bar{r}_p^2} \right) \right] \cdot (1 + \bar{r}'^2) \quad (6)$$

where  $k = \frac{E_2(1 + \nu_{21})}{E_1(1 + \nu_{12})}$  is the anisotropic parameter of the composite material;  $E$  and  $\nu$  are moduli, and Poisson's ratios satisfy the following relationship  $E_1 \cdot \nu_{12} = E_2 \cdot \nu_{21}$ .

- Fitting equation of dome profile: The dome meridian specified by equation (6) often has an inflection point where the direction of the curvature changes [7]. To obtain the full dome profile of the pressure vessel, we need a fitting equation having the following form [7]:

$$\begin{cases} \left( \bar{z} + \bar{R}_{1f} \cdot \sin \alpha_f - \bar{z}_f \right)^2 + \left( \bar{r} + \bar{R}_{1f} \cdot \cos \alpha_f - \bar{r}_f \right)^2 = \bar{R}_{1f}^2 \\ \alpha_f = \arccos \left( (1 + \bar{r}^2)^{-1/2} \right) \Big|_{\bar{z} = \bar{z}_f} \end{cases} \quad (7)$$

where the subscripts  $f$  denotes the fitting point;  $\bar{R}_1$  is the dimensionless meridional radius;  $\alpha$  is the angle between the radial radius and the parallel radius.

## 2.2. Composite laminate thickness on the dome

### 2.2.1. Tsai–Wu failure criterion

As analyzed in the section “Introduction”, in this study, the Tsai-Wu failure criterion will be used to predict the laminate thickness of the dome. The expanded form of the Tsai-Wu criteria is as follows [9]:

$$F_1 \cdot \sigma_1 + F_2 \cdot \sigma_2 + 2 \cdot F_{12} \cdot \sigma_1 \cdot \sigma_2 + F_{11} \cdot \sigma_1^2 + F_{22} \cdot \sigma_2^2 + F_6 \cdot \tau_{12} + F_{66} \cdot \tau_{12}^2 \leq 1 \quad (8)$$

where  $\sigma_1$  and  $\sigma_2$  are derived by the relations (4) and (5), which are expressed as equations (9) and (10);  $\tau_{12}$  is zero based on the optimized condition [4];  $F_i$  and  $F_{ij}$  are the strength parameters determined by the relations (11).

- Expressions for  $\sigma_1$  and  $\sigma_2$ :

$$\sigma_1 = \frac{m \cdot \bar{N}_\theta - n \cdot \bar{N}_\varphi}{\bar{h}} \quad (9)$$

$$\sigma_2 = \frac{m \cdot \bar{N}_\varphi - n \cdot \bar{N}_\theta}{\bar{h}} \quad (10)$$

in which  $m = \frac{\sin^2 \beta}{\sin^2 \beta - \cos^2 \beta}$  and  $n = \frac{\cos^2 \beta}{\sin^2 \beta - \cos^2 \beta}$ .

- Expressions for  $F_i$  and  $F_{ij}$ :

$$F_1 = \left( \frac{1}{X_1^T} - \frac{1}{X_1^C} \right), F_2 = \left( \frac{1}{X_2^T} - \frac{1}{X_2^C} \right), F_{12} = -\frac{1}{2} \cdot \sqrt{\frac{1}{X_1^T \cdot X_1^C \cdot X_2^T \cdot X_2^C}}, \quad (11)$$

$$F_{11} = \frac{1}{X_1^T \cdot X_1^C}, F_{22} = \frac{1}{X_2^T \cdot X_2^C}, F_6 = \left( \frac{1}{X_{12}^T} - \frac{1}{X_{12}^C} \right), F_{66} = \frac{1}{X_{12}^T \cdot X_{12}^C}$$

in which  $X_1^T$ ,  $X_1^C$ ,  $X_2^T$  and  $X_2^C$  stand for the tensile and compressive strengths of the unidirectional layer in the longitudinal and transverse directions of the filament;  $X_{12}^T$  and  $X_{12}^C$  are the positive and negative shear strength of laminate (the solver usually considers  $X_{12}^T = X_{12}^C$ ).

### 2.2.2. Objective function of thickness at the equator of the dome

By substituting equations (9) and (10) into the relation (8) and taking the equal sign, as well as referring to equations (2) and (3), we get the following one:

$$f(\bar{h}) = a_1 \bar{h}^2 - b_1 \bar{h} - c_1 = 0 \quad (12)$$

in which  $a_1 = 1$ ;  $b_1$  and  $c_1$  are coefficients determined as the below ones.

$$b_1 = F_1 \cdot (m \cdot \bar{N}_\theta - n \cdot \bar{N}_\varphi) + F_2 \cdot (m \cdot \bar{N}_\varphi - n \cdot \bar{N}_\theta) \quad (13)$$

$$c_1 = 2 \cdot F_{12} \cdot (m \cdot \bar{N}_\theta - n \cdot \bar{N}_\varphi) \cdot (m \cdot \bar{N}_\varphi - n \cdot \bar{N}_\theta) + F_{11} \cdot (m \cdot \bar{N}_\theta - n \cdot \bar{N}_\varphi)^2 + F_{22} \cdot (m \cdot \bar{N}_\varphi - n \cdot \bar{N}_\theta)^2 \quad (14)$$

Equation (12) is the second-order equation having the product of  $a_1$  and  $c_1$  to be

negative. Thus, it always exists a positive root corresponds to the material thickness  $\bar{h}$ . From the relations (13) and (14), we also see that  $b_l$  and  $c_l$  depend on the dimensionless radial distance  $\bar{r}$  and the winding angle  $\beta$ . It means that  $b_l$  and  $c_l$  depend on the dimensionless axial coordinate  $\bar{z}$ . Therefore, for a determined dome shape, at an arbitrary point assigned on the dome, we will receive a value  $\bar{h}(\bar{z})$  evaluated by solving equation (12).

Now, to determine the material thickness at the equator and thickness distribution on the dome, we need two assumptions (1)- the number of all the fibers crossing any plane is constant; and (2)- the fiber volume fraction is maintained consistently. Since those, we have:

$$\bar{h} = \bar{h}(\bar{z}) = \bar{h}_{eq} \cdot \frac{\cos \beta_{eq}}{\bar{r}(\bar{z}) \cdot \cos \beta(\bar{z})} \quad (15)$$

where  $\bar{h}_{eq}$  is the dimensionless material thickness at the equator.

As above-analyzed, for each determined thickness of  $\bar{h}(\bar{z})$ , we will derive a certain value of  $\bar{h}_{eq}$  from equation (15); Thus, the final thickness at the equator will be the maximum of all values of  $\bar{h}_{eq}$  expressed as follows:

$$\bar{h}_{eq \max} = \max_{0 \leq \bar{z} \leq \bar{z}_p} \left[ \bar{h}(\bar{z}) \cdot \frac{\bar{r}(\bar{z}) \cdot \cos \beta(\bar{z})}{\cos \beta_{eq}} \right] \quad (16)$$

### 2.2.3. Prediction of thickness on the dome

Equation (16) can fairly describe the shell thickness in the distance  $\bar{r}_{2\bar{w}} = \bar{r}_p + 2\bar{w} \leq \bar{r} \leq 1$  [10], where  $\bar{w}$  is the dimensionless width of the fiber tape,  $\bar{w} = w/R$  ( $w$ - The tape width). In the vicinity of the polar hole,  $\bar{r}_p \leq \bar{r} \leq \bar{r}_{2\bar{w}}$ , we should use a smooth approximation in the form of a third-order polynomial as follows [10]:

$$\bar{h}_a(\bar{z}) = a_2 \bar{z}^3 + b_2 \bar{z}^2 + c_2 \bar{z} + d_2 \quad (17)$$

where  $a_2$ ,  $b_2$ ,  $c_2$ , and  $d_2$  are coefficients determined by the following conditions:

- The function  $h(\bar{z})$  (including  $h_a(\bar{z})$ ) is continuous and has a continuous derivative at  $(\bar{r}_{2\bar{w}}, \bar{z}_{2\bar{w}})$ , i.e.,

$$\bar{h}(\bar{z}_{2\bar{w}}) = \bar{h}_a(\bar{z}_{2\bar{w}}) \quad (18)$$

$$\bar{h}'(\bar{z}_{2\bar{w}}) = \bar{h}'_a(\bar{z}_{2\bar{w}}) \quad (19)$$

- The material volume calculated by equations (15) and (17) for  $\bar{r}_p \leq \bar{r} \leq \bar{r}_{2\bar{w}}$  is similar, i.e.,

$$2\pi \int_{\bar{z}_{2\bar{w}}}^{\bar{z}_p} \bar{r}(\bar{z}) \cdot \bar{h}(\bar{z}) \cdot \sqrt{1 + \bar{r}'(\bar{z})^2} d\bar{z} = 2\pi \int_{\bar{z}_{2\bar{w}}}^{\bar{z}_p} \bar{r}(\bar{z}) \cdot \bar{h}_a(\bar{z}) \cdot \sqrt{1 + \bar{r}'(\bar{z})^2} d\bar{z} \quad (20)$$

- At the polar hole, the material thickness,  $\bar{h}_p$ , is given, i.e.,

$$\bar{h}_a(\bar{z}_p) = \bar{h}_p \quad (21)$$

According to Vasiliev [2], the thickness,  $\bar{h}_p$  should be chosen in accordance with a particular process. For free winding with fiber tapes uniformly distributed over the shell equator without overlap,  $\bar{h}_p = 2\bar{h}_{eq}$ ; in case of restriction induced by the polar boss,  $\bar{h}_p$  depends on the tape width and can change from  $5\bar{h}_{eq}$  up to  $10\bar{h}_{eq}$ . The above four expressions are enough to find coefficients  $a_2, b_2, c_2$ , and  $d_2$ .

### 2.3. Geometric constraints

To solve equations (6) and (7) for determining the dome profile and equations (12), (15), and (16) for obtaining the material thickness at the equator, we must have some geometric constraints as follows:

- Continuity condition: At the equator ( $\bar{z} = 0$ ),  $\bar{r} = 1$  and  $\bar{r}' = 0$ ; and at the polar point ( $\bar{z} = \bar{z}_p$ ),  $\bar{r} = \bar{r}_p$ ;
- Convexity condition: For  $0 \leq \bar{z} \leq \bar{z}_p$ ,  $\bar{r}'' \leq 0$ ;
- Side condition:  $0 \leq \bar{r} \leq 1$ .

## 3. RESULTS AND DISCUSSION

In this section, we will give some calculation results from using theoretical formulas in the section 2 for three common composite materials having mechanical properties, as in table 1.

**Table 1.** Mechanical properties of some unidirectional composite materials [8].

Properties	Glass/ epoxy	Carbon/ epoxy	Aramid/ epoxy
Longitudinal modulus, $E_1$ (GPa)	60	140	95
Transverse modulus, $E_2$ (GPa)	13	11	5.1
Poison's ratio, $\nu_{21}$	0.3	0.27	0.34
Longitudinal tensile strength, $X_1^T$ (MPa)	1800	2000	2500
Longitudinal compressive strength, $X_1^C$ (MPa)	650	1200	300
Transverse tensile strength, $X_2^T$ (MPa)	40	50	30
Transverse compressive strength, $X_2^C$ (MPa)	90	170	130
In-plane shear strength, $X_{12}$ (MPa)	50	70	30
Anisotropic parameter, $k$	0.265	0.098	0.071

Fig. 3. shows the dome profiles corresponding to three composite materials and the polar radius,  $\bar{r}_p = 0.2$ . It can be found that the bigger the parameter,  $k$ , the higher the dome height. The dome profiles designed for two composite materials, carbon/epoxy and aramid/epoxy, are almost similar. Fig. 4. shows the effect of the polar radius,  $\bar{r}_p$  on the material thickness at the equator,  $\bar{h}_{eq\max}$ . It is easy to see that the increase in the polar radius,  $\bar{r}_p$ , causes the material thickness at the equator to increase, the rate of thickness increase is greater when increasing the polar radius,  $\bar{r}_p$ . Due to the influence of the

strength parameters of the materials, the thickness at the equator of the aramid/epoxy shell is the smallest, followed by the carbon/epoxy shell and finally the glass/epoxy shell.

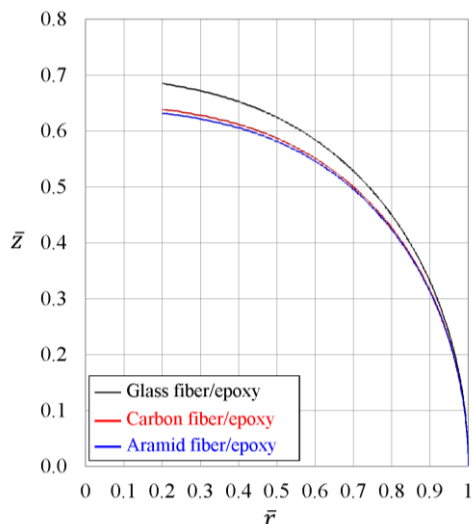


Figure 3. Dome profiles corresponding to three composite materials and  $\bar{r}_p = 0.2$ .

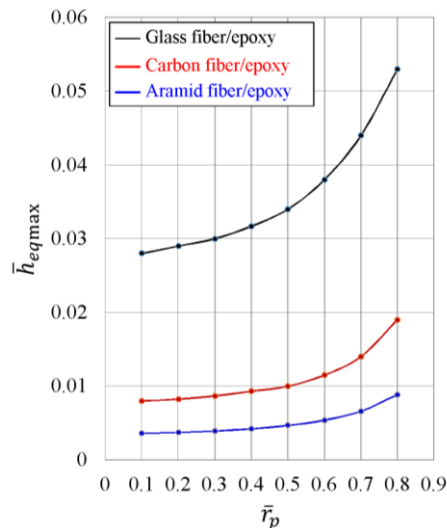


Figure 4. Effect of  $\bar{r}_p$  on  $\bar{h}_{eq\max}$  with  $p = 10$  MPa and  $\bar{w} = 0.1$ .

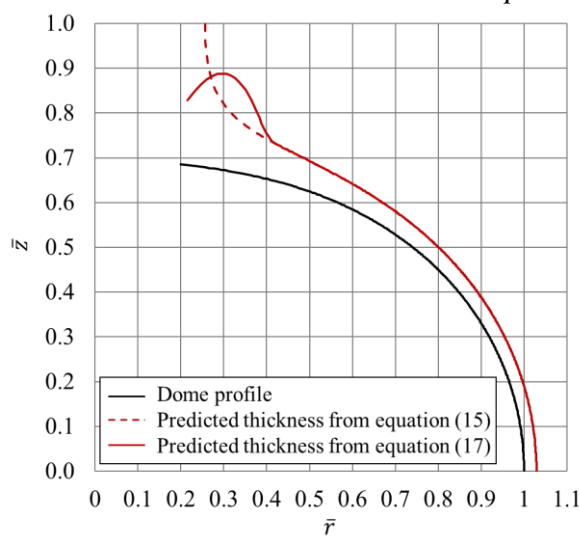


Figure 5. Predicted material thickness on the dome (material: glass/epoxy,  $\bar{r}_p = 0.2$  and  $\bar{h}_p = 5\bar{h}_{eq}$ ).

Prediction of the distribution of the material thickness on the dome for the glass/epoxy material, the polar radius,  $\bar{r}_p = 0.2$  and the material thickness at the polar hole,  $\bar{h}_p = 5\bar{h}_{eq}$ , is shown in Fig. 5. It can be observed that the material thickness distribution predicted from equation (15) – dashed line, is not realistic due to slipping, realignment, roving separation of the fiber tows, and material consolidation in the process of winding and curing. The material thickness predicted by using equation (17) – solid line, seems more realistic. This has certain significance in developing composite pressure vessels using the above method and incorporating finite element analysis.

#### 4. CONCLUSIONS

Continuum theory (lamination theory) and Tsai-Wu's multi-axial failure criterion of the composite material were utilized in the calculation of structural parameters of the geodesic wound composite pressure vessel, in which, the problem of determining the laminate thickness and predicting the material thickness on the dome were applied in this study. The current study is purely theoretical, but it is useful for the analysis, design, and determination of actual winding processing parameters of the composite pressure vessel.

#### REFERENCES

- [1]. C. C. Liang et al., "Optimum design of dome contour for filament-wound composite pressure vessels based on a shape factor", Composite Structures 58, (2002).
- [2]. V. V. Vasiliev et al., "New generation of filament-wound composite pressure vessels for commercial applications", Composite Structures 62, (2003).
- [3]. L. Zu et al., "Design of filament-wound domes based on continuum theory and non-geodesic roving trajectories", Composites: Part A 41, (2010).
- [4]. Đinh Văn Hiến và Trần Ngọc Thanh, "Biên dạng đáy vỏ trụ composite dị hướng nhận được bằng phương pháp quần trắc địa", Hội nghị KH toàn quốc về CHVR lần thứ XV, (2021), (in Vietnamese).
- [5]. J. S. Park et al., "Analysis of filament wound composite structures considering the change of winding angles through the thickness direction". Composite Structures 55 (1), (2002).
- [6]. R. M. Jones, "Mechanics of composite materials", McGRAW-Hill Co, (1975).
- [7]. Dinh Van Hien et al., "Design of planar wound composite vessel based on preventing slippage tendency of fibers", Composite Structures 254, (2020).
- [8]. V. V. Vasiliev and E. V. Morozov, "Advanced mechanics of composite materials", UK: Elsevier Ltd, (2007).
- [9]. S. W. Tsai and E. M. Wu, "A general theory of strength for anisotropic materials", J Compos Mater 5(1), (1971).
- [10]. A. A. Krikanov, "Refined thickness of filament wound shells", Science and Engineering of Composite Materials 10 (4), (2002).

#### TÓM TẮT

##### **Dự báo chiều dày vật liệu trên đáy của bình áp lực composite dị hướng được quần trắc địa**

Bình áp lực composite được thiết kế dựa trên việc xem xét vai trò của nền đến cân bằng lực của kết cấu và rò rỉ của bình do phá hủy của nền, cụ thể là trạng thái ứng suất và biến dạng của vỏ được xét đồng thời theo cả phương dọc và ngang sợi. Do điều kiện tải như vậy, việc dự báo chiều dày lớp composite của vỏ không dùng tiêu chuẩn ứng suất chính lớn nhất như với bình composite đơn hướng truyền thống mà cần dùng tiêu chuẩn phá hủy đa trục của vật liệu composite. Với các nền tầng đã phát triển và công bố về thiết kế biên dạng đáy vỏ bình áp lực composite, bài báo này trọng tâm vào dự báo chiều dày lớp vỏ composite trên đáy của bình áp lực được quần trắc địa theo tiêu chuẩn phá hủy Tsai-Wu, đồng thời tiên đoán phân bố chiều dày vật liệu trên đáy để làm cơ sở cho xác định các tham số kết cấu của bình.

**Từ khóa:** Chiều dày lớp composite; Bình áp lực composite; Composite dị hướng; Quần trắc địa.